PROLOGUE

This report seeks to answer some of the questions raised during the practical training course organized within the framework of ARCAL-RLA-6042-IAEA project "Early diagnosis of Helicobacter pylori infection by means of nuclear techniques" undertaken in Hermosillo, México, during the first week of November 2003. We include some general aspects of Helicobacter pylori infection as well as the current method for the determination of $^{13/12}CO_2$ ratio in exhaled air to detect the presence of this bacterium in the gastric mucosa, the Urea Breath Test (^{13}C-UBT). We hope that this manual will be useful and understandable for the interested reader. Any doubts suggestions, corrections and questions will be welcomed and answered with pleasure.

The authors

ARCHIVOS LATINOAMERICANOS DE NUTRICION
Organo Oficial de la Sociedad Latinoamericana de Nutrición
Vol. 54 Supl N° 2, 2004

The usefulness of stable isotopes in nutrition and human health: the application of mass spectrometry and ^{13}C-breath tests to detect *Helicobacter pylori* infection

Barrado A.[1], Preston T.[2], Slater C.[3], Zubillaga M.[1], Miranda-da-Cruz B.[4], Mokhtar N.[4], Zednik M.[5], Valencia M.E.[6] and Boccio J.[1]

SUMMARY. The interest in *Helicobacter pylori* has escalated in recent years. *H. pylori* may produce a chronic gastric infection which is usually life-long and many epidemiological studies have shown that this is the most common bacterial infection throughout the world involving 50% of the world population. Thus, it is clear that the diagnosis of *H. pylori* infection represents at least a key step in the management of many of the patients referred to the gastroenterologist. Additionally, due to the wide range and relevance of pathologies possibly related tho this infection, from micronutrient malnutrition and co-infections to malignancies, there is the potential for *H. pylori* to be a major health problem. Improved methods for the diagnosis and follow up treatment of the infection have been developed. Use of stable isotopes as non-invasive and safe diagnostic methods, namely (^{13}C) breath tests, has been the key to a new era of research in *H. pylori* epidemiology and diagnosis as well as the establishment of eradication therapies. This non-invasive nuclear technique, that is considered the gold standard for the diagnosis of this bacterial infection, has successfully been standardized and implemented along Latin America. Taking into account the high prevalence of this bacterial infection, the impact of this technique in the whole region is very high. In this article we discuss several aspects of this methodology in order to harmonize the application of this method in developing regions.

Key words: *Helicobacter pylori*, UBT, diagnosis, stable isotope, mass spectrometry.

RESUMEN. Utilidad de los isótopos estables en salud humana y nutrición: espectrometría de masas y test de aliento con ^{13}C-urea aplicados a la detección de infección por *Helicobacter pylori*. El interés en investigación en el área de *Helicobacter pylori* se ha incrementado en los últimos años. La infección por *H. pylori* puede producir gastritis crónica a lo largo de toda la vida. Varios estudios epidemiológicos han demostrado que esta infección bacteriana es la de mayor prevalencia en el mundo, afectando el 50% de la población mundial. Asi, es claro que el diagnóstico de la infección por *H. pylori* representa un paso clave en el manejo de los pacientes que acuden al gastroenterólogo. Asi mismo, debido al amplio rango de patologías relacionadas con la infección por esta bacteria que van desde la deficiencia de micronutrientes a procesos neoproliferativos, demuestran el potencial efecto nocivo que puede provocar la infección por *H. pylori* en la salud humana. En los últimos años se han mejorado significativamente los métodos de diagnóstico. El uso de isótopos estables, especialmente los denominados prueba del aire exhalado, como métodos seguros y no invasivos, han sido un paso clave en una nueva era de investigación dedicada al diagnóstico como asi también en la elección de las terapias de erradicación para *H. pylori*. Esta técnica nuclear no invasiva, que actualmente es considerada método de referencia para la determinación de la infección por *H. pylori*, ha sido exitosamente implementada en América Latina. Teniendo en cuenta la elevada prevalencia de la infección por *H. pylori* , el impacto de la implementación de esta metodología en la región es muy alto. En este artículo se discute en forma detallada los aspectos de esta metodología para armonizar la aplicación de este método diagnóstico en las regiones en vías de desarrollo.

Palabras clave: *Helicobacter pylori*, UBT, diagnóstico, isótopos estables, espectrometría de masas.

[1]Stable Isotope Laboratory Applied to Biology and Medicine. Physics Department. School of Pharmacy and Biochemistry. University of Buenos Aires. Argentina.
[2]Stable Isotope Biochemistry Laboratory. Scottish Universities Environmental Research Centre. East Kilbride. Glasgow. United Kingdom.
[3]University of Glasgow. Division of Developmental Medicine. Yorkhill Hospitals. Glasgow. United Kingdom.
[4]Section of Nutritional and Health-Related Environmental Studies. Division of Human Health. International Atomic Energy Agency. Vienna. Austria.
[5]Latin-American Section. Department of Technical Cooperation. International Atomic Energy Agency. Vienna. Austria.
[6]Research Center for Food and Development. Hermosillo. Mexico.

INTRODUCTION

The interest in *Helicobacter pylori* has escalated in recent years. *H. pylori* may produce a chronic gastric infection which is usually life-long and many epidemiological studies have shown that this is probably one of the most common bacterial infections throughout the world involving 50% of the world population. Thus, it is clear that the diagnosis of *H. pylori* infection represents at least a key step in the management of many of the patients referred to the gastroenterologist.

Additionally, due to the wide range and relevance of pathologies possibly related to this infection, from micronutrient malnutrition and co-infections to malignancies, there is the potential for *H. pylori* to be a major health problem. Improved methods for the diagnosis and follow up treatment of the infection have been developed. Use of stable isotopes as non-invasive and safe diagnostic methods, namely [^{13}C] breath tests, has been the key to a new era of research in *H. pylori* epidemiology and diagnosis as well as the establishment of eradication therapies.

Helicobacter pylori

H. pylori is a Gram-negative, spiral shaped, microaerophilic bacterium isolated from human gastric mucosa that produces large amounts of urease, an enzyme that hydrolyses urea into carbon dioxide and ammonia.

There are two identified patterns of infection for *H. pylori*. In the first instance, developing countries have a large proportion of children infected during early life and almost all adults are colonised. Studies showed a prevalence of approximately 13-70% in subjects between 0-20 years of age and 70-94% in those older than 30. The second pattern is characterized by the increase in the prevalence of *H. pylori* infection from 20 years onwards, and it is typical of developed countries with values of 5-15% prevalence in children and 20-60% in individuals between 30-75 years of age. Thus, it is accepted that *H. pylori* infection is disseminated worldwide, with an average prevalence of 50%. There is also an inverse relationship between the prevalence of the infection and the socioeconomic status of the population concerned.

This bacterium may produce chronic antral gastritis, peptic ulcer and is associated with stomach cancer. *H. pylori* carriers are up to 15 times more likely to develop duodenal ulcers than *H. pylori* negative individuals. The predominant infections and concomitant inflammation in duodenal and gastric ulcers tend to occur in the antrum and corpus, respectively. The most convincing evidence that *H. pylori* is a key pathogen in peptic ulcer disease is the observation that its eradication dramatically reduces the ulcer recurrence rate. The hypothetical cascade of events in the pathogenesis of duodenal ulcer initiates with the infection causing inflammation in the mucosa. This leads to alterations of regulatory hormones with the net effect of acid hypersecretion. The duodenal mucosa reacts to acid hypersecretion with the formation of gastric metaplasia, which in turn allows *H. pylori* to colonize the duodenum. The final event of mucosal breakdown is caused by several facultative factors. In the long time interval between initial infection and the occurrence of intestinal-type gastric carcinoma, data suggest that *H. pylori*-associated chronic gastritis evolves through atrophy, intestinal metaplasia and dysplasia. Many factors involved in *H. pylori* virulence have been studied in detail, including urease, the vacuolating cytotoxin (Vac A), the product of cytotoxin-associated gene A (Cag A), the neutrophil-activating protein (NapA) and lipopolysaccharide. Bacterial adhesion to the mucosal surface is an initial important step for colonization and infection. On the other hand, it is widely accepted that *H. pylori* adheres to receptors in the gastric epithelium by means of specific adhesins. This is a topic worthy of further investigation to clarify mechanisms of *H. pylori* colonization and the possibility of developing new strategies for treatment.

H. pylori has also been linked to micronutrient malnutrition. Even though nutrient absorption does not take place in the stomach, this organ contributes to the process by means of the secretion of hydrochloric acid and enzymes, which during the digestive process, help not only to release the micronutrients from the food matrix but also, in the case of the essential minerals, to render them soluble. Achlorhydria (a decrease of hydrochloric acid secretion) occurs in 40-50% *H. pylori* infected patients. A consequence of which is poor absorption of micronutrients, which may compromise the nutritional status of infected individuals provoking the appearance of deficiency symptoms.

Stables isotopes in nutrition and metabolic research

Nuclear techniques have been used to determine dynamic aspects of metabolism in both animals and humans. Isotopes can be radioactive or stable, and the latter allows the use of them in vulnerable groups, such as pregnant women and children where radioactive isotopes may have an unacceptable medical risk. The global nutrition community has recognized the significance of isotope techniques, especially utilizing stable isotopes, as providing accurate and non-invasive methods for measuring nutrient assimilation, nutrient status and related metabolism. As investigative tools, stable isotopes are now seen to be invaluable, since there is virtually no health risk involved in their use. They are therefore preferred for work in humans, especially infants and pregnant women. They can be administered either orally or intravenously and when incorporated into metabolic products, such as body water, urea or CO_2, they can be easily sampled in saliva, milk, breath, urine and stool.

^{13}C breath tests are based on the delivery of a ^{13}C-labelled substrate into the body by oral ingestion or by injection. A specific enzyme in the target tissue then selectively metabolizes the substrate such that the tracer is irreversibly released as $^{13}CO_2$ into the body's bicarbonate pool. The tracer is then transported by the circulation and exhaled in the breath. The pattern of breath $^{13}CO_2$ enrichment over time can be measured. The isotope analysis can be performed by isotope-ratio mass spectrometry (IRMS).

^{13}C-breath tests are mainly used as research tools, but they can be applied successfully in less privileged countries, as they are simple to perform and can be reliably used to evaluate gastrointestinal function. The test can be presented in a kit, which can be used in all members of the population. Breath samples can be stored unaltered in economical collection tubes (e.g., Exetainers) for up to six months before being sent to a centralized analytical laboratory by standard mail.

The urea breath test to detect the presence of *H. pylori* in the stomach is the simplest breath test. The high urease activity by *H. pylori* has facilitated the development of diagnostic methods using either ^{14}C-urea or ^{13}C-urea, which are hydrolysed to labelled CO_2 and exhaled. These methodologies have the advantage of representing the whole stomach surface and of being non-invasive. Until now, several invasive endoscopic methods have been used in the diagnosis of the gastric infection by *H. pylori* including histology, culture, rapid urease test and polymerase chain reaction. None of these can be considered a reference method since samples obtained by endoscopy are focal in nature and do not represent the whole stomach surface.

In this report, we will describe and discuss some methodological aspects related to the diagnosis of *Helicobacter pylori* infection by mass spectrometric analysis of the $^{13/12}CO_2$ ratio in exhaled breath.

^{13}C-urea breath test (^{13}C-UBT)

The ^{13}C-urea breath test is used to diagnose *H. pylori* infection. In this test, ^{13}C-urea is administered orally in a test meal (commonly natural orange juice), and urease secreted by *H. pylori* in the stomach acts hydrolyses urea to release $^{13}CO_2$. $^{13}CO_2$ then enters into the body's bicarbonate pool and is excreted in breath. Breath $^{13}CO_2$ enrichment can be measured by IRMS. An increase in breath enrichment of $^{13}CO_2$ within 45 minutes of the ingestion of ^{13}C-urea is indicative of the presence of *H. pylori* in the gastric mucosa.

Methodology as performed in Latin America

- Fasting for 6 hours.
- Basal samples in duplicate.
- Intake of 50-100 mg of ^{13}C-urea in test meal (natural orange juice).
- Breath samples at 30 and 45 min after ^{13}C-Urea intake.
- Measurement of the breath samples by IRMS.

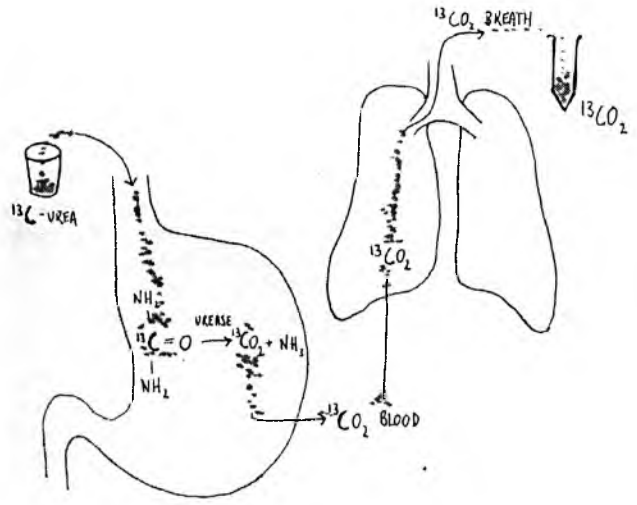

Materials: (Fig. 1) A few materials are needed to perform the test, they are:

- 50-100 mg of ^{13}C-urea.
- Test meal: natural orange juice.
- Straw
- Four Exetainers: two for the basal samples (red cap) and two for 30 and 45 minutes post ^{13}C-urea intake (blue cap).

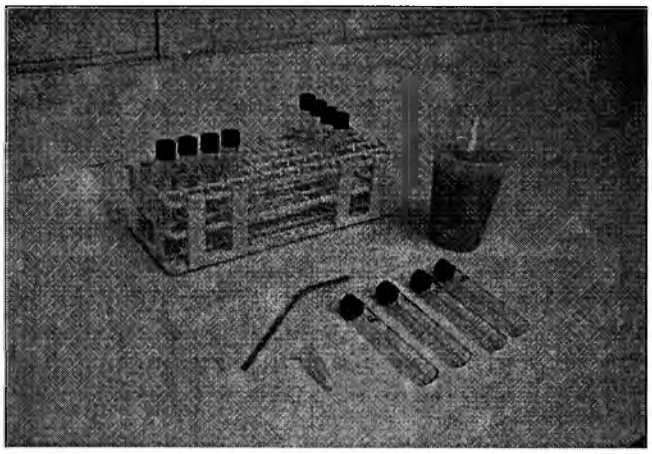

FIGURE 1

Addition of the ^{13}C-urea into the test meal (Fig. 2).

The ^{13}C-urea is easily dissolved in the test meal by stirring. It does not alter the taste of the meal.

FIGURE 2

Teeth brushing (Fig. 3).

Teeth should be cleaned before ingestion of the ^{13}C-urea test meal to decrease the potential interference of bacteria in dental plaque.

It should be done without toothpaste, using only water.

FIGURE 3

Basal breath samples (Fig. 4),

Basal breath samples should be taken in duplicate to determine the basal $^{13/12}CO_2$ ratio using the Exetainer with red cap.

Breath should be sampled by blowing through a straw into the Exetainer

FIGURE 4

^{13}C-urea- test meal intake (Fig. 5).

The whole test meal containing the ^{13}C-urea dose must be taken.

FIGURE 5

Teeth brushing (Fig. 6).

Teeth should be brushed after consumption of the ^{13}C-urea test meal to wash out any residual^{13}C-urea in the oral cavity where bacteria may show urease activity, which would interfere with the test. Clean teeth without using toothpaste. Use only water.

FIGURE 6

30 minute breath sample (Fig. 7).

Use the Exeteiner with the blue cap.

Breath should be sampled by normal-deep breath blowing into the Exetainer through the straw.

FIGURE 7

45 minute breath sample (Fig. 8).

Use the Exeteiner with the blue cap.

Breath should be sampled by normal-deep breath blowing into the Exetainer through the straw.

FIGURE 8

Breath samples for measuring (Fig. 9),

Each breath sample is identified by means of a bar-code label. Samples can be kept at room temperature for up to 6 months. They could be submitted to a central laboratory by standard mail.

FIGURE 9

The basal value is determined in duplicate and then samples are collected 30 and 45 minutes after the ingestion of approximately 250 cm^3 of natural orange juice to which 50 mg of urea enriched with ^{13}C are added. This form of administration delays gastric emptying of the labelled urea and favors contact with the whole gastric mucosa. This is important for the sensitivity of the method since *Helicobacter pylori* does not colonize the whole gastric mucosa but only patches.

Mass spectrometry

The mass spectrometer, the cyclotron and the J.J. Thompson device are based on the interaction of electric and magnetic fields with ions, i.e., electrically charged atoms or molecules. In 1887 J.J. Thompson at Cambridge (England) measured for the first time the electron charge/mass ratio using a vacuum glass tube in which a bundle of electrons is pulled out of the cathode and accelerated to a screen covered with a fluorescent substance that indicates the impact site. Lawrence and Stanley Livingston of California University discovered the cyclotron in 1931. This consists of two metallic chambers in the shape of the letter D, in which it is possible to produce a pulse of atomic particles with high speed.

Conceptually, mass spectrometry is the separation of ions, which are produced and separated or filtered according to their mass/charge ratio (m/z) and finally detected. Many different instruments have been developed using this principle. Breath ^{13}C enrichment is measured using an isotope ratio mass spectrometer (IRMS). The first gas source IRMS was designed by Alfred Nier in 1947 (1).

Recent advances, especially in sample introduction technology, have increased the efficiency, sensitivity and specificity of this technique through the introduction of continuous-flow IRMS by Preston and co-workers (2,3,4). In continuous flow instruments, CO_2 is separated from the other components of breath, in a helium stream, by gas chromatography. Water is removed and the pure CO_2 is carried into the IRMS, eliminating the need for off-line sample preparation. The addition of an autosampler and computer controlled instrumentation lead to the first fully automated system for analysis of breath $^{13}CO_2$ enrichment (5). Other advances include introduction of user-friendly software, allowing the spread of IRMS instrumentation to many laboratories around the world.

Isotopes

Isotopes are forms of an element of differing mass that have the same number of protons (and therefore electrons), the difference being the number of neutrons.

Electrons are responsible for their chemical behavior and therefore isotopes cannot be differentiated by chemical reactions, but as the number of neutrons is different their mass will be different.

The accepted nomenclature to designate a nuclide is

$$^{A}_{Z}X$$

X: nuclide; **A:** mass number (A = Z + N); **Z:** atomic number, i.e., the number of protons; **N:** number of neutrons.

Isotopes of the same chemical element have the same Z and differ in A. In ^{13}C breath tests, we need to consider the isotopes present in CO_2 in the breath sample.

Table 1 shows the percent composition of C and O of their stable species, i.e., their **isotopic abundance**.

Table 1

Atom	Isotope	Isotopic abundance (%)
C	^{12}C	98.89
	^{13}C	1.108
	^{14}C	Very low
O	^{16}O	99.76
	^{17}O	0.04
	^{18}O	0.2

The elements contain **stable** or **radioactive isotopes.**

In the case of carbon, we find two stable isotopes, ^{12}C and ^{13}C and one radioactive isotope, ^{14}C. The three isotopes of oxygen shown in the table are stable.

It should be noted that the quantity of ^{13}C naturally present in a human being weighing 70 kg is approximately 120 g. Thus, if 50 mg ^{13}C-urea (~11mg ^{13}C) is given for a breath test, this is scarcely 0.01 per cent of the total.

Several molecular species of CO_2 can be formed by combining different isotopes.

These molecules of CO_2 correspond respectively to masses 44, 45, 45 and 46.

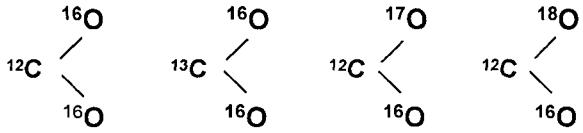

The probability of finding theses ions among those formed in exhaled breath depends upon the isotopic abundance of the elements. Other CO_2 molecules, which could be formed by combining two or more minor isotopes, have a very low probability of being formed. The intensity of ions at mass 44 will be some 90-fold greater than that of other masses, due to the contribution of $^{12}C^{16}O_2$ formed by the most abundant isotopes.

Isotope Ratio Mass Spectrometry

A number of IRMS designed specially for automated analysis of ^{13}C breath tests are commercially available. The photograph (Fig. 10) shows the equipment installed at the Laboratory of Stable Isotopes applied to Biology and Medicine, School of Pharmacy and Biochemistry, University of Buenos Aires, which is a Finnigan BreathMAT (Thermo Electron Corporation, Tel: Africa +27 11 570 1840, UK +44 1442 233555; www.thermo.com). Although this instrument is no longer commercially available, in principle, its design and operation are similar to other instruments.

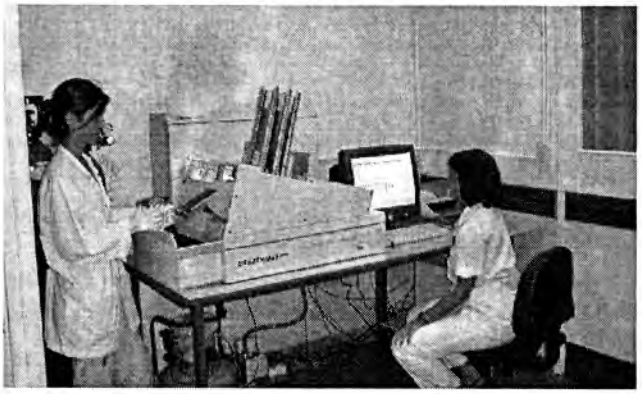

FIGURE 10

The components of the BreathMAT can be seen (from left to right) in Figure 10.

1. He and CO_2 cylinders (partially obscured by an operator).
2. On the table: the mass spectrometer, the autosampler, the monitor and the printer.
3. Under the table: compressor, rotary vacuum pump and computer CPU (partially obscured).

The procedure for the diagnosis of infection by *H pylori* using the ^{13}C-urea breath test is described step-by-step (pag. 29-31).

Following sample collection as described above, the analytical procedure begins with **identification** by affixing self-adhesive labels with a bar code on the tubes and the location of the tube into the autosampler magazine (Fig. 11). In each batch, up to10 magazines with 20 tubes each may be located.

Once the bar code has been read by the **laser reader**, the autosampler makes the maneuvers destined to that the tube is punctured by the **needle** (Fig. 11).

The breath sample is displaced of the tube by means of a helium current that enters by the needle. The needle has two concentric routes. The helium is introduced through the central route, and the breathed air sample enters the needle by a lateral orifice and is carried to the IRMS by the same helium flow. Once extracted the sample, the tube is pushed towards a box but if for some reason, the laser reader cannot read the bar code, it is derived to a **sorter ramp** (Fig. 11) where is ordered according to the sequence of measurement of the samples.

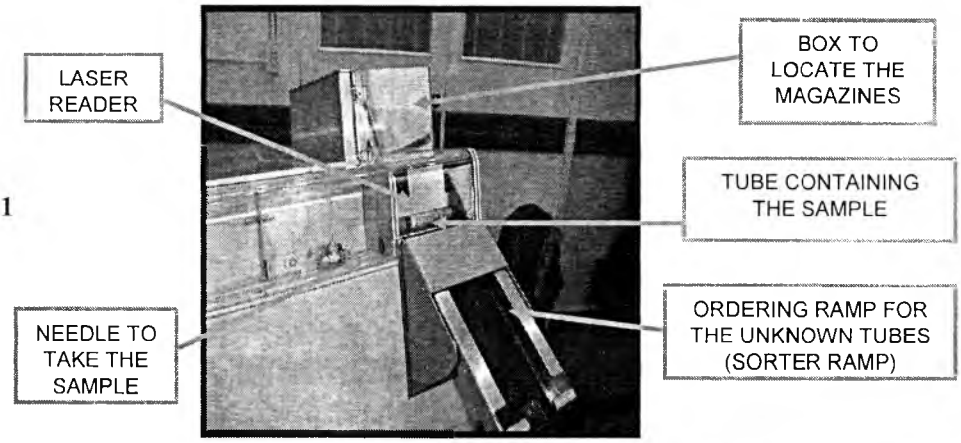

FIGURE 11

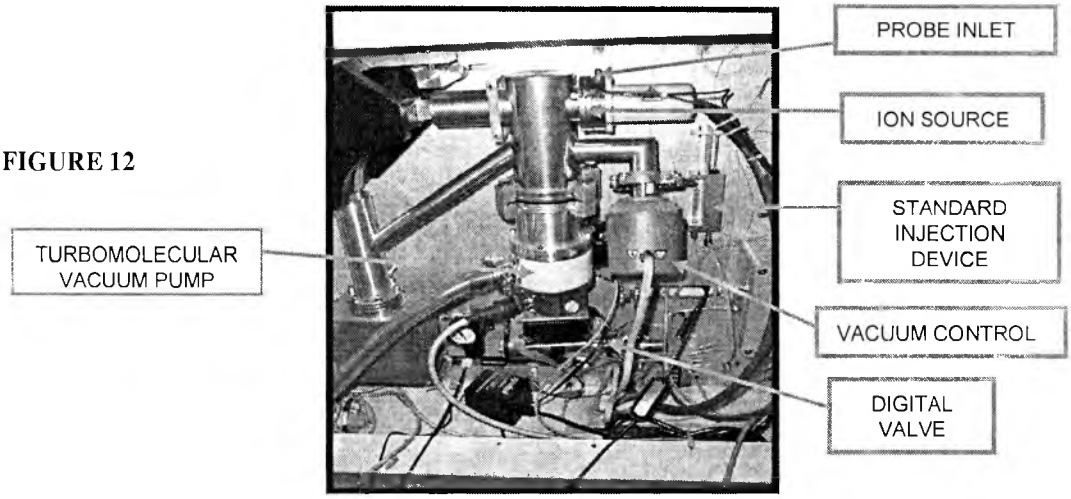

FIGURE 12

The breath sample is transported in a stream of helium to an eight-way **VALCO digital valve** (Fig. 12). This valve has two positions: "load" and "Inject". In the Load position, the sample fills a 2 mL **loop**. A turn of the valve to the Inject position causes the loop contents to flow towards the **gas chromatograph** (GC) (Fig. 13). A new turn brings the valve back to the Load position and, while the loop is filled, the flow is maintained through the GC. The valve turns are controlled by the computer software at predetermined times.

The breath sample mainly contains: oxygen, nitrogen, water vapor and carbon dioxide.

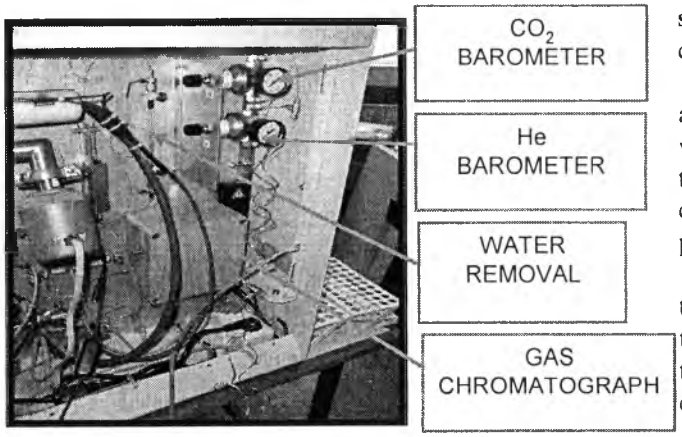

FIGURE 13

Gases entering the GC are separated. **Water removal** (Fig. 13) is accomplished by a permeable membrane. The flow now passes through an element called the **Standard Injection Device** (Fig. 12), the function of which is to alternate pulses of sample and reference gas.

Gases enter the **ion source** (Fig. 12), in which high vacuum conditions prevail, produced by the **turbomolecular vacuum pump** (Fig. 14) backed by the rotary pump.

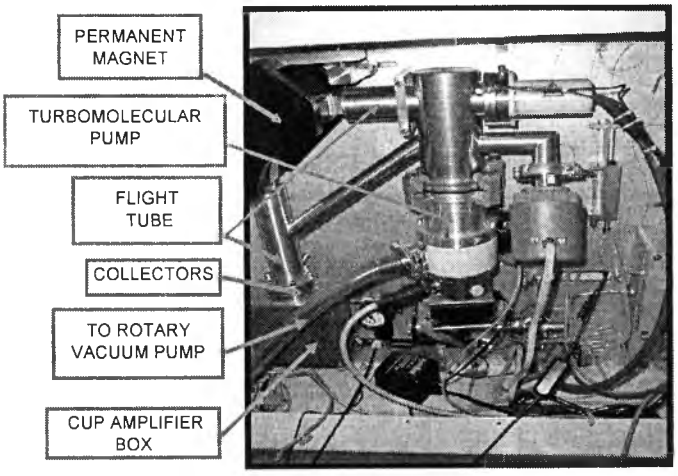

FIGURE14

In the ion source there is a **tungsten filament** that emits electrons, which ionize a small portion of the CO_2 transforming it into a positive ion, CO_2^+.

$$CO_2 + 1\ e^- \rightarrow CO_2^+ + 2\ e^-$$

Ions are formed following thermionic emission of electrons from the filament and their collision with gas molecules. Two small permanent magnets within the ion source increase the probability of collision with a CO_2 molecule as they cause the electrons to describe a spiral from the filament. The **emission** of electrons is under strict electronic control to maintain constant ionization efficiency.

In the ion source there is a **high vacuum**, 10^{-6} mbar (the atmospheric pressure is almost 1,000,000,000 times higher!!!), which is produced by two vacuum pumps, a mechanical rotary backing pump and a turbomolecular (high vacuum) pump connected in series. In this way the necessary high mean free path for the ions is achieved.

The CO_2^+ ions produced are accelerated through a potential difference of approximately 3000 Volts (accelerating potential). The energy of the electric field produced by this potential difference is transferred to the ions and its value can be calculated easily (see Appendix 2).

The Finnigan BreathMAT spectrometer is an IRMS, which is a low resolution magnetic sector MS, and so has no velocity selector as it will be described in Appendix 1. Ions with different mass enter the magnetic field, where they describe different radii.

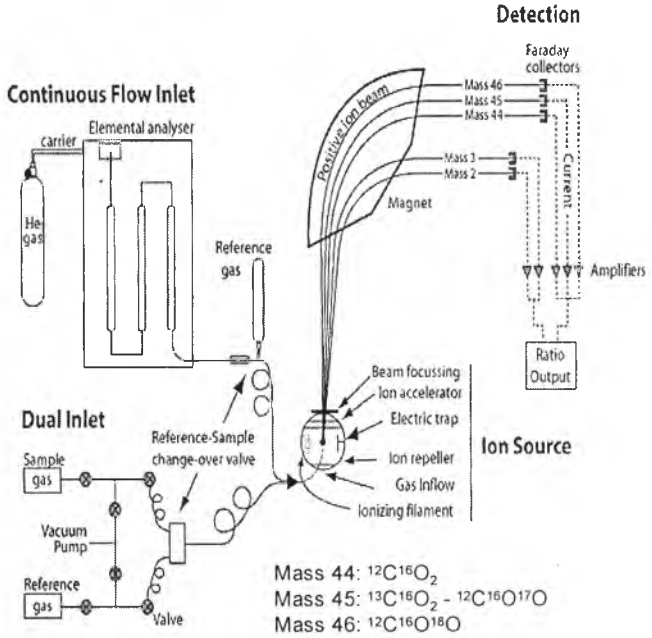

FIGURE 15

The IRMS is designed to monitor ions of mass-to-charge-ratio 44, 45 and 46. The detectors are ion collectors called **Faraday cups** (Fig. 15). The different isotopic abundances produce currents with different intensities in each detector (**cup1**, **cup2** and **cup3**). Therefore, each amplifier gain is optimised (by the value of the resistor installed) so that those receiving the less abundant ions (corresponding to masses 45 and 46) have ~100-fold more gain than that corresponding to mass 44 (**cup 1**).

Data Analysis

IRMS results are expressed as current intensity ratios (the $^{13}CO_2/^{12}CO_2$ ratio is termed ratio 45 in the Breath MAT software). Simultaneous collection of the isotopic species cannot be affected by variations of the total ion amounts arriving at the collectors, since intensity ratios and not their absolute values are determined. Processing includes comparison of the ratio 45 (actually 45/44) of the sample with the ratio 45 of the CO_2 reference gas, which has a known carbon isotopic composition relative to the international standard for carbon isotopic composition (notation $\delta\ ^{13}C$; units ‰, per mil). The original international standard, a limestone called **Pee Dee Belemnite** (**PDB**) has been exhausted, but a new primary standard has been produced (6). This new standard is known as Vienna PDB (VPDB).

The delta value of the reference gas has been entered into the software, which now automatically undertakes a series of corrections to account for the contribution of ^{17}O to mass 45 in the calculation of R45/44 (the Craig correction, see scheme below). The result is now calculated as $\delta^{13}C$ relative to the reference gas (**Del 13**), which is then converted to $\delta^{13}C$ relative to PDB (**Del 13 PDB**). The final result of every sample is determined by the difference between the **Del 13 PDB of the sample** after the ingestion of ^{13}C-UREA and the **basal Del 13 PDB**. The difference is called DOB (Delta Over Baseline, Δ). The results of ^{13}C breath tests can also be expressed in units of part per million (ppm) ^{13}C and ppm ^{13}C excess (7).

The precision of analysis becomes poorer at lower than desirable CO_2 concentration. When the ion current falls below a pre-determined minimal value the software produces a "**low signal**" message. In these cases the DOB data that the sheet gives automatically should be neglected. Low CO_2 concentration is usually the result poor sample collection, which may be due to failure to replace the cap on the Exetainer correctly

The results of the determinations appear on a sheet similar to that shown here (Table 2).

Table 2

Sample	Barcode	Name	Remarks	DOB	Del 45	Del 46	Ratio 45	Ratio 46	Del 13	Del 13 PDB	mV
Basal	52100	NICOLAS		0.0	5.1	-1.6	1.2	0.4	5.5	-22.6	2398
30 min	52100		Positive	47.3	50.7	1.3	1.2	0.4	54.1	24.7	1980
Basal	52130			0.0	4.8	-0.8	1.2	0.4	5.2	-22.9	2478
45 min	52130		Positive	31.3	35.1	4.3	1.2	0.4	37.3	8.4	1664
Basal	52200	ULISES		0.0	7.1	-4.3	1.2	0.4	7.7	-20.5	2502
30 min	52200		Positive	57.2	62.5	8.3	1.3	0.4	66.4	36.7	604
Basal	52230			0.0	7.0	-4.6	1.2	0.4	7.6	-20.5	2414
45 min	52230		Positive	41.6	47.3	-0.7	1.2	0.4	50.5	21.2	2634
Basal	52300	MARCOS		0.0	9.0	-2.1	1.2	0.4	9.7	-18.5	2477
30 min	52300		Negative	1.5	10.5	-1.8	1.2	0.4	11.3	-17.0	2317
Basal	52330			0.0	6.9	-6.9	1.2	0.4	7.6	-20.5	2922
45 min	52330		Negative	2.2	9.2	-2.6	1.2	0.4	9.9	-18.3	2643

The value of the cut-off point of the test is a DOB higher than 3.5, i.e., once the DOB of a sample is higher than 3.5 the result will be POSITIVE (8).

Several columns are not shown and the values have been rounded to one decimal place to show those of most interest. In the second column the number, which identifies each patient, is indicated. A signal indicates when a bar code reading has been carried out and the system inscribes the number in this column. If the signal from the bar code reader is not received, the Exetainer will be put on the ordering ramp once the sample has been analysed. The legend **"Unknown"** will appear in the output followed by the number indicating the

sequence order. When this occurs for the tenth time, the batch will be terminated since the ordering ramp will be full. In this eventuality sample identities are entered into the spreadsheet manually in the order indicated by the position of the tube on the ramp and the number. The column "mV" contains the values corresponding to a signal generated in the detector of the ions of mass 44 (of the isotope $^{12}C^{16}O^{16}O$), the most abundant. These values act as a quality control because the signal measured should be higher than the predetermined threshold value.

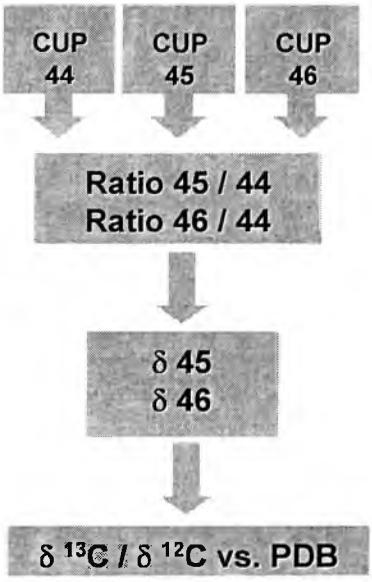

The schematic diagram shows the series of steps that together comprise the measurement of the $^{13}C/^{12}C$ ratio in the sample and in the reference gas.

Ratio 45 and 46: The ratios established between the signal intensities

$$R\ 45\ /\ 44\ = \frac{^{13}C^{16}O_2 + ^{12}C^{17}O^{16}O + ^{12}C^{16}O^{17}O}{^{12}C^{16}O_2} =$$

$$= {}^{13}R45/44 + 2*{}^{17}R45/44$$

The data appearing with the notation δ (delta), are generally results of a relationship with the reference gas:

$$\delta^{13}C(^{o}/_{oo}) = \left[\left(R_{sample} / R_{reference}\right) - 1\right] * 10^{3}$$

Del 45: $$\delta 45 = \frac{(\text{ratio } 45/44_{sample} - \text{ratio } 45/44_{ref.})}{\text{ratio } 45/44_{ref.}} * 1000\ (^{o}/_{oo})$$

Del 46: $$\delta 46 = \frac{(\text{ratio } 46/44_{sample} - \text{ratio } 46/44_{ref.})}{\text{ratio } 46/44_{ref.}} * 1000\ (^{o}/_{oo})$$

Del 13: The result of correction for the ^{17}O contribution to mass 45 in the calculation of R45/44. The correction proposed by Craig includes two constants (Craig A and Craig B), determined experimentally (9).

$$\delta^{13}C = CraigA * \delta 45 - CraigB * \delta 46$$

$$\delta^{13}C = 1.0676758 * \delta 45 - 0.0338362 * \delta 46$$

Routine quality control checks

In all routine IRMS operations, regular QC checks are undertaken. Peak centering is undertaken to ensure that the high voltage is adjusted to optimize ion beam focus; a stability test is undertaken to ensure that any variation of isotope ratio with time is within acceptable limits; a reproducibility or analytical precision test is undertaken to ensure precision is acceptable and that 'zero enrichment' criteria are met. Somewhat less frequently, an abundance sensitivity test (sometimes called amount dependence or linearity) is performed to ensure that any variation of measured ratio with sample size is within accepted limits.

In the Finnigan BreathMAT, routine QC tests are known as:

1) High voltage; 2) Time scan; 3) CO_2zero _20

1- High Voltage Scan (Fig. 16).

A reference gas peak is scanned over a 10 V range in HT to find the optimal accelerating voltage. Once automatically selected it should prove stable for the ratio 45/44 (<1 V per kV) in a constant temperature environment (18°C).

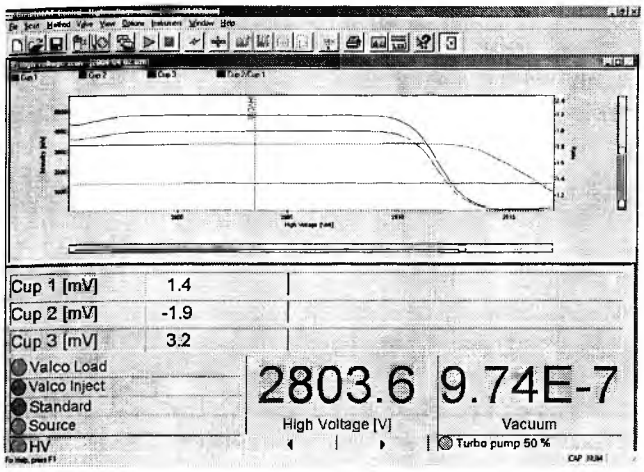

FIGURE 16

2- Time scan (Fig. 17).

A reference gas peak is monitored over 10 minutes, at the previously selected accelerating voltage. A variation of <1 per thousand in ratio 45/44 over 10 minutes is acceptable.

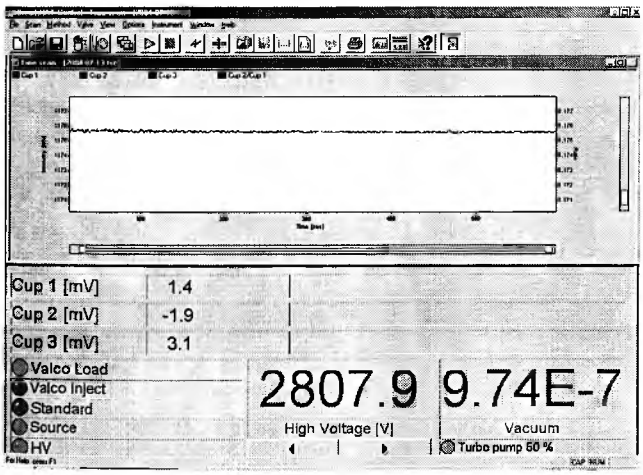

FIGURE 17

3- CO_2 zero_20

This test is performed by undertaking 20 measurements of reference gas. The standard deviation of the Del 13 PDB values is calculated by means of an Excel sheet. The result should not be greater than 0.07 per mil. The purpose of this control is to check the reproducibility of the determinations. The data from this test are transferred automatically to a sheet which can be exported to Excel (Table 3).

Table 3

No.	Del 45	Del 46	Ratio 45	Ratio 46	Del 13	Del 13 PDB	mV
1	-0.16	-0.05	1.18	0.42	-0.17	-28.06	3108.20
2	-0.12	-0.08	1.18	0.42	-0.13	-28.03	3105.40
...							
19	0.00	0.01	1.18	0.42	0.00	-27.90	3076.50
20	0.02	-0.07	1.18	0.42	0.02	-27.88	3143.90
						0.05	

The value of 0.05 $^{o}/_{oo}{}^{13}C$, at the end of the Del13PDB column corresponds to the standard deviation of the 20 preceding values. The test is satisfactory.

Other breath tests in human health

The 1-^{13}C-octanoic acid breath test for solid phase gastric emptying

This test of solid phase gastric emptying is described in full by Ghoos and co-workers (10,11). Unlike the case with the UBT, where data is expressed in units of enrichment, the convention has been to convert the IRMS data from the octanoic acid breath test into units of percentage dose recovered (PDR), where,

$$\text{PDR h}^{-1} = \frac{\text{VCO}_2 \text{ (mmol h}^{-1}\text{) x breath } ^{13}\text{CO}_2 \text{ enrichment (ppm excess) x 100}}{\text{amount substrate taken (mmol) x substrate enrichment (atom \% excess x } 10^4\text{)}}$$

Note that many IRMS data systems only yield data in δ ^{13}C units (7). As it is more convenient to deal with tracer dose in units derived from atom fraction (atom % excess, or ppm excess), it may be necessary to interconvert units of enrichment (7).

A modest dose (typically 100 µl) of 1-^{13}C-labelled octanoic acid is incorporated into the test meal (usually within egg yolk) and cooked. The subject remains seated and at rest. They give a baseline breath sample and take the test meal. A series of breath samples are given over a 6 hour period. The full protocol is available on the SIGN website (www.med.rug.nl/sign).

The Figure 18 shows the output from a solid phase gastric emptying test. Use of the curve fitting procedure advocated by Ghoos and co-workers (10,11) revealed in this case a gastric emptying half time of 2.8 hours. Calculations such as these that may involve data manipulation and curve fitting are greatly facilitated by use of spreadsheets. All the IRMS manufacturers provide data outputs that can be readily imported into proprietary spreadsheets, such as Microsoft Excel.

^{13}C-octanoic acid breath test

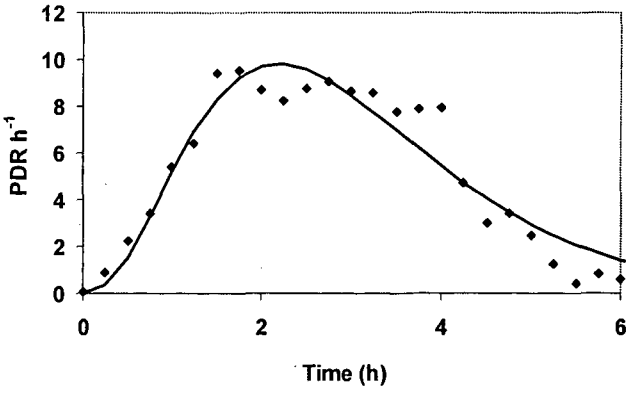

FIGURE 18

The main outcome of the octanoic acid breath test is a kinetic measurement, typically gastric emptying half time. Strictly speaking, this information could have been calculated from the plot of tracer enrichment with time, without having to convert it to PDR. However it is essential to express the outcome in PDR units in certain breath tests (see below).

The study above was performed using an AP2003 isotope ratio mass spectrometer system designed for automatic analysis of ^{13}C breath tests. This IRMS is currently manufactured by: GV Instruments, Crewe Road, Wythenshawe, Manchester M23 9BE, UK (tel: +44 (0) 161 9022100; fax: +44 (0) 161 9022198; http://www.gvinstruments.co.uk).

The ^{13}C-mixed triacylglycerol breath test for pancreatic lipase sufficiency

Here a novel molecule, the mixed triacylglycerol (1,3 distearyl 2-[1-^{13}C]octanoyl-glycerol), was designed and developed by Ghoos and co-workers (12,13), to detect maldigestion due to insufficient secretion of pancreatic lipase. This is now available commercially (www.isotope.com). The triacylglycerol is incorporated into a test meal and consumed. A series of breath samples taken, as in the octanoic acid breath test. When the tracer is fully digested, the unlabelled stearic acid moities are removed from the *sn*-1 and *sn*-2 positions by pancreatic lipase. The resulting monoacylglycerol or nonesterified fatty acid is readily absorbed and transported to the liver where it is oxidised, releasing $^{13}CO_2$, which is exhaled in breath. Subjects with insufficient pancreatic lipase secretion give low recovery of ^{13}C in breath CO_2 (14).

Mixed triacylglycerol breath test

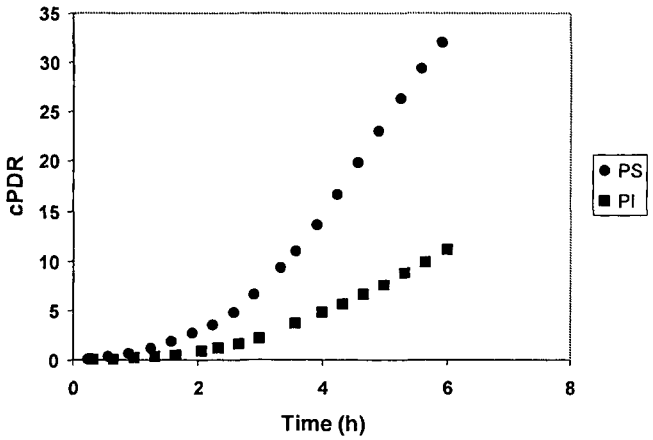

FIGURE 19

The Figure 19 shows the cumulative PDR (cPDR) in breath CO_2 following a mixed triacylglycerol breath test in children with cystic fibrosis (●pancreatic sufficient, PS; ■ pancreatic insufficient, PI). This test has been successfully applied to assess the need for digestive enzyme supplementation in children with cystic fibrosis (15-17). Here, accurate measures of PDR are essential (18).

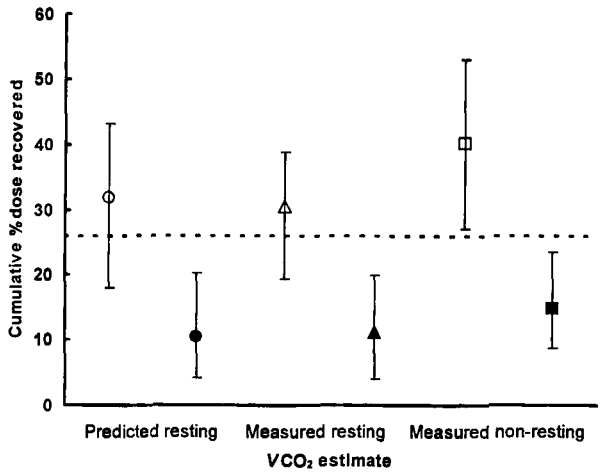

FIGURE 20

This Figure 20 illustrates the importance of obtaining accurate estimates of CO_2 production to yield accurate cPDR data. Non-resting VCO_2 estimates, from heart rate, were used to calculate cPDR over 6 h during the mixed triacylglycerol breath test. Open symbols are the median cPDR from pancreatic sufficient subjects (n = 19, shown with range). Closed symbols are the median cPDR from children with cystic fibrosis, who have been prescribed pancreatic enzyme replacement therapy, but did not take PERT with the test meal (n = 5, shown with range).

These studies were performed using a Europa ABCA isotope ratio mass spectrometer system designed for automatic analysis of ^{13}C breath tests. This IRMS is currently manufactured by: SerCon Ltd, Wistaston Road Business Centre, Wistaston Road, Crewe, Cheshire CW2 7RP, UK (Tel: +44-(0)1270-580008;Fax:+44-(0)1270-252310;http://www.sercongroup.com)

ACKNOWLEDGEMENTS

We would also like to thank the IAEA for supporting the Hermosillo training course and for giving us the opportunity to participate and the motivation for this work. Finally we would like to express our appreciation to our host, the Research Centre for Food and Development.

REFERENCES

1. Nier AO. A mass spectrometer for routine isotope abundance measurements. *Review of Scientific Instruments* 1940;11,212-216.
2. Preston T & Owens NJP. Interfacing an automatic elemental analyser with an isotope ratio mass spectrometer: the potential for fully automated total nitrogen and nitrogen-15 analysis. *Analyst* 1983;108, 971-977.
3. Preston T & Owens NJP. Preliminary ^{13}C measurements using a gas chromatograph interfaced to an isotope ratio mass spectrometer. *Biomedical Mass Spectrometry* 1985;12, 510-513.
4. Preston T & McMillan DC. Rapid sample throughput for biomedical stable isotope tracer studies. *Biomedical and Environmental Mass Spectrometry* 1988;16, 229-235.
5. Prosser SJ, Brookes ST, Linton A & Preston T. Rapid, automated analysis of ^{13}C and ^{18}O of CO_2 in gas samples by continuous-flow, isotope ratio mass spectrometry. *Biological Mass Spectrometry* 1991;20,724-730.
6. Coplen TB. New guidelines for reporting stable hydrogen, carbon, and oxygen isotope-ratio data. *Geochimica et Cosmochimica Acta* 1996;60, 3359-3360.
7. Slater C, Preston T & Weaver LT. Stable isotopes and the International System of Units. *Rapid Communications in Mass Spectrometry* 2001;15, 1270-1273.
8. Slater C, Preston T, Weaver LT. Is there an advantage in normalising the results of the *Helicobacter pylori* [^{13}C]urea breath test for CO_2 production rate in children? *Isotopes in Environmental and Health Studies* 2004;40, 89-98.
9. Craig H. Isotopic standards for carbon and oxygen and correction factors for mass-spectrometric analysis of carbon dioxide. *Geochimica et Cosmochimica Acta* 1957;12, 133-149.
10. Maes BD, Ghoos YF, Rutgeerts PJ, Hiele MI, Geypens BJ & Vantrappen G. [*C]octanoic acid breath test to measure gastric emptying rate of solids. *Digestive Diseases and Sciences* 1994;39, 104S-106S.
11. Maes BD, Mys G, Geypens BJ, Evenepoel P, Ghoos YF & Rutgeerts PJ. Gastric emptying flow curves separated from carbon-labeled octanoic acid breath test results. *American Journal of Physiology* 1998;275, G169-G175.
12. Ghoos YF, Vantrappen G, Rutgeerts PJ & Schurmans PC. A mixed-triglyceride breath test for intraluminal fat digestive activity. *Digestion* 1981;22, 239-247.
13. Vantrappen GR, Rutgeerts PJ, Ghoos YF & Hiele MI. Mixed triglyceride breath test: a noninvasive test of pancreatic lipase activity in the duodenum. *Gastroenterology* 1989;96, 1126-1134.
14. Amarri S & Weaver LT. ^{13}C-breath tests to measure fat and carbohydrate digestion in clinical practice. *Clinical Nutrition* 1995;14,149-154.
15. Amarri S, Harding M, Coward WA, Evans TJ & Weaver LT. ^{13}Carbon mixed triglyceride breath test and pancreatic enzyme supplementation in cystic fibrosis. *Archives of Disease in Childhood* 1997;76, 349-351.
16. de Boeck K, Delbeke I, Eggermont E, Veereman-Wauters G & Ghoos Y. Lipid digestion in cystic fibrosis: comparison of conventional and high lipase enzyme therapy using the mixed-triglyceride breath test. *Journal of Pediatric Gastroenterology and Nutrition* 1998;26, 408-411.
17. van Dijk-van Aalst K, Van Den Driessche ML, van der Schoor S, Schiffelers S, Van't Westeinde T, Ghoos Y & Veereman-Wauters G. ^{13}C mixed triglyceride breath test: a noninvasive method to assess lipase activity in children. *Journal of Pediatric Gastroenterology and Nutrition* 2001;32, 579-585.
18. Slater C, Preston T, & Weaver LT. Use of calibrated heart rate monitors to estimate CO_2 production rate during the ^{13}C-mixed triacylglycerol (MTG) breath test. *Proceedings of the Nutrition Society* 62, 9A. 2003.

APPENDIX 1

A short introduction to a few basic physical concepts such as circular motion and magnetic fields will help to understand the reasons for the separation of isotopes in a sample of exhaled breath to quantify the isotope ratio.

1. Circular motion

When an ion moves in a magnetic field in such a way that the direction of the **velocity** vector is perpendicular to the **magnetic induction** vector, its trajectory is a circumference.

FIGURE 21

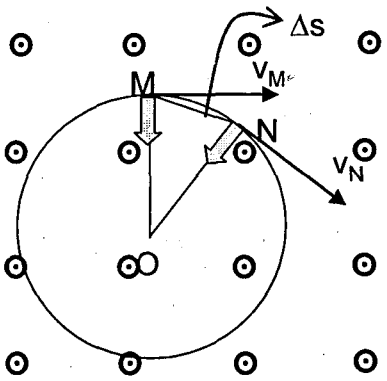

In the Figure 21 we consider a moving positive charge at two points M and N of its trajectory. The magnetic field is perpendicular to the paper and comes out of the paper sheet.
The grey vector represents the **force**, which the magnetic induction **B** exerts on the electric charge moving with a velocity **v**. The direction of the velocity is **tangent** to the trajectory at every point. The vectors entering into the paper may be represented by ⊗ (the tail of the arrow), and those coming out by ⊙ (the heat of the arrow)

When the label appears in **bold script** it refers to a vector; in normal script it refers to its velocity and direction.

This situation may be compared to that of a stone attached to a rope. The stone remains in a circular trajectory as long as the tension of the rope is maintained. If the rope is broken, the stone will move with a rectilinear trajectory with a direction coincident to that of the velocity vector at the moment of the break of the rope. In the case of the stone the involved forces are **contact forces** since they are transmitted by the rope; in the mass spectrometer the forces are transmitted by a field through a **distance**.

In the Figure 21 the vectors $\mathbf{v}_M$ **and** $\mathbf{v}_N$ represent tangential instantaneous velocities at M and N respectively.

Tangential velocity is defined as the quotient between the traveled arc and the time employed for the travel; in a more rigorous way it should be defined as the limit of the quotient between Δs y Δt when Δt tends to zero. Under these circumstance the arc may be taken as having the same length as Δs; therefore the first definition makes sense. The Greek letter Δ is used to symbolize change, in this case the "increase of" the variable which follows. It replaces the difference between the final and the initial values of the variable during the considered interval.

If we move the vectors representing the speeds to a common origin we can find the difference vector (Δ**v**) between $\mathbf{v}_M$ and $\mathbf{v}_N$ (Figure 22).

FIGURE 22

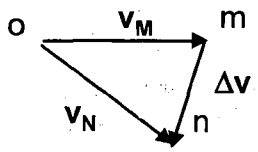

In order to understand these considerations, we may represent the difference between two vectors as the sum of $\mathbf{v}_M$ and Δ**v**. Then:

$$\mathbf{v}_M + \Delta\mathbf{v} = \mathbf{v}_N \quad \text{resulting} \quad \Delta\mathbf{v} = \mathbf{v}_N - \mathbf{v}_M$$

Conceptually the velocity change (Δ**v**) as a function of time is the acceleration. If we take the point N closer and closer to M, with time tending to zero, it will be:

d**v**/dt = **a** the direction and sense of **a** will be equal to that of d**v**

As points M and N are sufficiently close, Δ**v** becomes perpendicular to **v** and consequently the acceleration **a** as well. Therefore the acceleration at each point of the trajectory has a direction coincident to the radius and the sense is to the center. For this reason it is called **centripetal acceleration** and since the relationship with the force is the mass of the body (with positive sign), obviously the force producing this acceleration is coincident in sense and direction to that of the acceleration; we symbolize it in grey in Figure 21 and it is called **centripetal force.** This force is responsible for the change of direction of the tangential velocity.

We note that the effects of the forces may produce changes of the velocity which do not affect its modulo. If this is not so, it is required that the force has a component in the direction of the velocity and this is not the case in uniform circular motion.

The tangential velocity is a property that characterizes circular motion. It is very simple to infer that this tangential velocity is strongly dependent on the radius (distance at which the moving body is found with regard to the center of the circumference of the trajectory which it is describing). It is necessary to find a mathematical relationship between these variables.

When a body turns around a point it will "sweep" an angle. In a circular motion, angles are measured in "radians". An angle of 1 radian is defined when it subtends an arc equal to the length of the radius. Thus, an angle of 360° corresponds to an arc equal to the length of the circumference.

If we want to establish the equivalence between the hexadecimal system and the radian, we can take into account this relationship and since a **measurement is a comparison with the unit**, we should refer the arc (the length of the circumference) to the value of the radius.

360° is equivalent to $\frac{2 * \pi * R}{R} = 2 * \pi$

Since the ratio between a length and another length has no unit, the radian is actually dimensionless, even though sometimes it is referred to by the word "radian" in order to have a reference to the system in which we are working.

For example an angle of 45° is equal to $\pi/4$ radians.

Another property that characterizes the circular motion is the **angular velocity**, which is represented by ω.

It is defined by the "swept" angle (given in radians) during a certain time.

Let us suppose that the "swept" angle between M and N of Figure 21 is θ. Then:

$\omega = \theta/t$ the unit of ω will be s^{-1}, provided θ is give in radians

The angular velocity ω is a vector. The foregoing expression allows the calculation of the module of the vector. The direction will be perpendicular to the plane of the trajectory, it passes through its center and its sense is given by the rules of the vector calculus. Later, as we are going to analyze magnetic fields, we shall develop in detail the manner by which we can determine the sense in these cases.

It is doubtless that the angular velocity and the tangential velocity (**v**) are related.

The tangential velocity is nothing but a certain length, in this case an arc, swept during a certain time.

$$v = arco / t \qquad (1)$$

In order to measure the length of this arc it should be taken into account that a certain angle measured in radians belongs to this arc.

If the angle is θ we can establish this proportionality:

$$\frac{arco}{\theta} = \frac{2 * \pi * R}{2 * \pi}$$

Simplifying: $arco / \theta = R \Rightarrow arco = \theta * R$

Replacing in **(1)**: $v = \frac{\theta * R}{t}$

Since $\theta / t = \omega$ $\qquad v = \omega * R$

This equation shows that the tangential velocity is directly proportional to the radius of the trajectory. Thus, for example, if a row of soldiers turns, those who are at the center practically remain at the same place (tangential velocity nearly zero) but those marching at the distal extreme have to move very quickly in order to not break the line. Notwithstanding, the angle described by all of them is the same, i.e., they have the same angular velocity.

In the Figures 21 and 22 the triangles OMN and omn are resembling because they are isosceles and the angles formed by equal sides are equals between them (two isosceles triangles are resembling if the angles are equals and the homologous sides are proportional).

Thus: $\frac{\Delta s}{R} = \frac{\Delta v}{v} \Rightarrow \Delta v = \frac{v * \Delta s}{R}$

$a = \Delta v / t \Rightarrow a = \frac{v * \Delta s}{R * t}$ but $\Delta s / t = v$

It results: $a = \frac{v * v}{R}$ and $a = v^2 / R \qquad (2)$

The expression **(2)** will be used in the forthcoming analysis.

2.- Magnetic Field

The **force** of **magnetic** (F) origin is directly proportional to the **charge** (q) of the ion, to its **velocity** (v) and to the magnetic field of **magnetic induction (B)**.
The mathematical expression by which it is possible to calculate the force is:

$$\mathbf{F = q.\ (v \times B)}$$

v x B being the vector product of both vectors; for this reason the result is also a vector.

The module of the vector **F** is: $F = q \times v \times B \times \sin \varphi$;

φ being the angle between both vectors.

In the case of the mass spectrometer, **v** and **B** are perpendicular and therefore $\sin \varphi = 1$.

By definition of the vector product, the direction of the vector **F** is perpendicular to the plane determined by **v** and **B**.

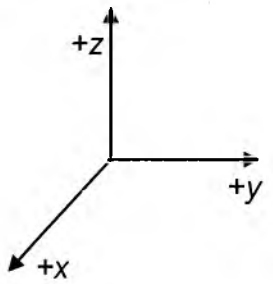

The sense of **F** will be determined operating mathematically. Assigning to each of the vectors **v** and **B** the senses of the cartesian coordinate axes +x and +y, respectively, the result for **F** is the sense +z.

In a practical way, the sense of **F** will be determined by the so called "right hand rule". The vector **B** "comes out" of the palm of the right hand, the fingers with the exception of the thumb should be pointed in the sense of the velocity. Separating the thumb at a right angle from the remaining fingers, the thumb will point in the sense of the force if the ion is positive. If the ion is negative the sense of the force will be opposite to that of the thumb.

There are more "familiar" ways to determine this result. If we overturn ("gyrate") **v** over **B** (with an angle smaller than 90°) the sense in which a corkscrew or a screw with a right coil would advance will give the sense of **F**.

The foregoing analysis shows that at the moment in which an ion penetrates perpendicularly into a magnetic field, a perpendicular force will begin to act by which the direction of the movement of the ion will change; the ion will be describing a circular trajectory.

When the ion leaves the magnet, the magnetic force will cease and therefore the ion will follow a straight trajectory, arriving to the zone of ion collection.

The module of the force is: $F = q \times v \times B$

The force is also $F = m \times a \Rightarrow m \times a = q \times v \times B$ (m = mass)

Since in this case the force is the centripetal force, the acceleration will be also centripetal.

*

According to equation **(2)**

$$a = v^2 / R \qquad \text{It results } \frac{m * v^2}{R} = q * v * B \Rightarrow$$

$$\frac{m * v}{q * B} = R \quad \Rightarrow R = \frac{v}{q * B} m$$

How can we read this equation? The radius described by an ion in a magnetic field depends on four variables: the velocity (**v**), the charge (**q**), the magnetic induction of the magnetic field (**B**) and the ion mass (**m**).

Two of these variables, the charge (**q**) and the magnetic induction (**B**) are similar for all the ions.

The Figure shows a scheme of a mass spectrometer, which has a **velocity selector**. This device allows the entrance into the zone of action of the spectrometer magnet of ions having only a determined value of its velocity.

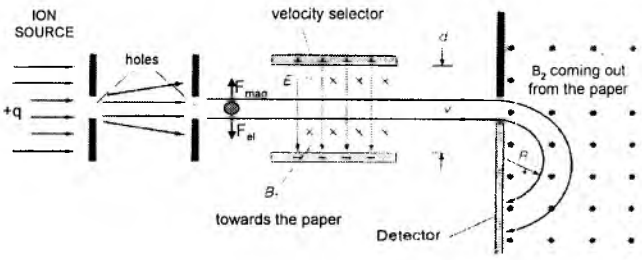

The ions, accelerated in an ion source, enter into a zone in which they interact with an electric field (**E**), which exerts an electric force ($\mathbf{F}_{el}$) on the ion in a sense downwards, and a magnetic field, perpendicular to the electric field and to the ion velocity, which exerts a magnetic force ($\mathbf{F}_{mag}$) in an opposite sense to the electric field. The electric field E is produced by two conducting plates submitted to difference of potential **V** and separated by a distance **d**.

The corresponding equations are:

$$\left.\begin{array}{l} F_{el} = q \cdot E \Rightarrow \quad F_{el} = q.V/d \\ F_{mag} = q.\, v \cdot B \end{array}\right\} \; v = \; V / B \cdot d$$

Since the forces $\mathbf{F}_{el}$ and $\mathbf{F}_{mag}$ are opposite, if their modules are equal, the ions with a velocity **v** would have a rectilinear uniform movement.

The ions with a higher velocity than V/(B.d) would move according to the sense of the magnetic force, whereas if their velocity would be smaller than this value, they would move in the sense of the electric force. In both cases they would not pass through a diaphragm located geometrically in the trajectory of the ions having velocity **v**.

Since isotopic compounds only differ in their nuclear masses, a mixture of isotopes with the same electric charge, the same velocity and moving in a zone with the same magnetic induction, will describe circular trajectories with different radii.

This is the reason that renders mass spectrometry a method of choice to determine the isotopic composition of an element in a sample.

APPENDIX 2

The energy of the ions can be calculated by taking into account that the electric charge of the ions is caused by the loss of one electron; since the charge of an electron is $-1.601864 \times 10^{-19}$ coulombs, it results:

$$\text{energy} = q \times V \Rightarrow \text{energy} = 1.601864 \times 10^{-19} \text{ coulomb} \times 3000 \text{ volt}$$
$$\text{energy} = 4.805592 \times 10^{-16} \text{ joule}$$

This energy is transferred as kinetic energy to the produced ions in the ion source.

In order to calculate the velocities acquired by the different isotopes of CO_2^+ taking into account that the kinetic energy, E_k, is equal to $m.v^2/2$.

$$v = \sqrt{\frac{2E_{cin}}{m}} \Rightarrow v = \sqrt{\frac{2 * 4{,}805592 * 10^{-16} J}{N * 1{,}67248 * 10^{-27} kg}} \Rightarrow v = \frac{758067{,}677}{\sqrt{N}} \frac{m}{s}$$

Replacing **N** for the mass values **44, 45 and 46** (which give the nucleon number), the following values for the velocities result:

V_{44} =114.283,0023 m/sec; V_{45} =113.006,0572 m/sec y V_{46} =111.770,982 m/sec

The calculations were carried out assigning a value of $1{,}67248 \times 10^{-27}$ kg to the nucleon mass (protons and neutrons). Strictly there is a mass difference between both nucleons but in this case this has been neglected. The mass of the electrons in each atom was also neglected since it can be estimated that the results are not changed. The velocity values are around 400.000 km/h.

APPENDIX 3

To calculate their radii we must first deduce a general equation, and then apply it to each isotope.

$$E_{cin} = \frac{1}{2}mv^2 \Rightarrow v = \sqrt{\frac{2E_{cin}}{m}} \quad \text{and since} \quad R = \frac{mv}{qB} \quad \text{it results}$$

$$R = \frac{m}{qB}\sqrt{\frac{2E_{cin}}{m}} \Rightarrow R = \frac{1}{B}\sqrt{\frac{m^2 2qV}{q^2 m}} \Rightarrow R = \frac{1}{B}\sqrt{\frac{2mV}{q}} \Rightarrow$$

$$R = \frac{1}{0{,}47 \text{ Tesla}}\sqrt{\frac{2 * N * 1{,}67248 * 10^{-27} kg * 3000 V}{1{,}601864 * 10^{-19} C}}$$

Where: Tesla is the unit of magnetic field intensity
N: number of nucleons
Mass of 1 (one) nucleon: $1{,}67248 * 10^{-27}$ kg
Acceleration potential difference of the ions:
V=3000 V
Intensity of the magnetic field:
B=4700 gauss = 0.47 tesla
Elemental charge: $q=1{,}601864 * 10^{-19}$ coulomb

Performing the operations we obtain:

$$\Rightarrow R = \frac{7{,}9148606 * 10^{-3} m}{0{,}47} * \sqrt{N}$$

Now we simply replace **N** for the values **44**, **45** and **46**.

$$R_{44} = 0{,}1117 \text{ m} \quad R_{45} = 0{,}1130 \text{ m} \quad R_{46} = 0{,}1142 \text{ m}$$

These values are coherent with the geometry of the spectrometer magnet. All the previous development may be summarized by the equation:

$\frac{m}{q} = \frac{B^2 * R^2}{2 * V}$ this expresses adequately the conditions of the spectrometer

In this expression the values of electric charge of the ions, **q**, the accelerating potential, **V** and the magnetic induction, **B** are the same for all the isotopes. Therefore, the radii of the trajectories, **R**, depend on the ion mass, **m**, which may be calculated as the mass of one nucleon multiplied by the number of nucleons of the isotope. Furthermore, **B** is a fixed value and **V** results from the selection of the maximal voltage.